

Interplay of Correlation, Randomness and Dimensionality Effects in Weakly-Coupled Half-Filled Random Hubbard Chains

JUN-ICHIRO KISHINE AND KENJI YONEMITSU
 Institute for Molecular Science, Okazaki 444-8585, Japan

We study interplay of electronic correlation, randomness and dimensionality effects in half-filled random Hubbard chains weakly coupled via an interchain one-particle hopping. Based on the two-loop renormalization-group approach, phase diagrams are given in terms of temperature vs. strengths of the intrachain electron-electron umklapp scattering, the random scattering and the interchain one-particle hopping.

Keywords: quasi-one-dimensional conductor; umklapp scattering; Mott insulator; randomness; Anderson localization

INTRODUCTION

Randomness effects in interacting electron systems have provoked a great deal of controversy over the past two decades. In the one-dimensional case away from half filling, Giamarchi and Schulz^[1] discussed strong interference between correlation-induced quantum fluctuations and random scattering processes, by applying the renormalization-group (RG) approach to the bosonized Hamiltonian obtained by the replica trick. Recently, Fujimoto and Kawakami^[2] discussed the case of half filling, where competition between the correlation-induced Mott transition and the randomness-induced Anderson localization arises. In quasi-one-dimensional systems, three dimensionality induced by an interchain coupling plays an important role^[3]. In half-filled Hubbard chains weakly coupled via an interchain one-particle hopping, t_{\perp} , without randomness, there occur the interchain one-particle propagation through the t_{\perp} - process and the propagation of the 1D antiferromagnetic (1DAF) power-law correlation through the interchain particle-hole exchange (ICEX) processes^{[3],[4]}. The former process drives a crossover to the Fermi liquid (FL) regime, while the latter process causes a transi-

tion to an antiferromagnetic (AF) phase from an incoherent metal (ICM) phase^[4]. In this paper, we study the randomness effects on the competition between them in weakly-coupled half-filled random Hubbard chains. We apply the two-loop RG approach to the effective action obtained by the replica trick. Instead of the bosonization technique^{[1],[2]} which takes account of only the collective degrees of freedom, we here use the effective action with Grassmann representation to treat both of the interchain one-particle (individual) and two-particle (collective) processes.

EFFECTIVE ACTION

We consider an array of the half-filled random Hubbard chains. In Figs.1(a)-1(e), we show all the fundamental processes included here. The intrachain one-particle propagation to the right- and left-directions [Figs.1(a-1) and (a-2), respectively] is treated by linearizing the one-particle dispersion at the Fermi points. Scattering of electrons by the weak random potential at a spatial position, x , is taken into account through a real field, $\eta(x)$, corresponding to random forward scattering [Fig.1(b-1)] and complex fields, $\xi(x)$ and $\xi^*(x)$, corresponding to random backward scattering [Fig.1(b-2)]. We assume the random potential to be governed by Gaussian distributions,

$$P_\eta \propto \exp \left[-D_\eta \int dx \eta(x)^2 \right], \quad (1)$$

$$P_\xi \propto \exp \left[-D_\xi \int dx \xi(x) \xi^*(x) \right], \quad (2)$$

where $D_\eta = (\pi N_F \tau_\eta)^{-1}$ and $D_\xi = (\pi N_F \tau_\xi)^{-1}$ with $\tau_{\eta,\xi}$ and N_F being the scattering mean free times and the noninteracting one-particle density of states, respectively. At half filling, the intrachain interaction generates the normal [Figs.1(c-1,2)] and umklapp [Fig.1(c-3)] scattering processes with dimensionless strengths, g_1 , g_2 and g_3 , for the backward, forward and umklapp scattering, respectively. Initial values of the intrachain scattering strengths are related to the on-site Coulomb repulsion, U , by $g_{1;0} = g_{2;0} = g_{3;0} = U/\pi v_F$ at half filling with v_F being the Fermi velocity. We here consider only the case of $g_{1;0} - 2g_{2;0} < |g_{3;0}|$, where the most dominant 1D power-law correlation is an antiferromagnetic one. Accordingly, the most dominant ICEX process is in the AF channel. Figures 1(d-1) and (d-2) show the interchain one-particle hopping (t_\perp) processes between the nearest-neighbor chains for the right- and left-moving electrons,

respectively. Multi- t_{\perp} - and g_i ($i = 1, 2, 3$)-scattering processes generate dynamically the interchain AF interactions during the renormalization. Their strengths in the normal and umklapp channels are denoted by J [Fig. (e-1)] and K [Fig. (e-2)], respectively.

FIGURE 1 Fundamental processes considered here. The solid and broken lines represent the propagators for the right- and left-moving electrons, respectively. The wavy lines represent the intrachain two-particle scattering (g_1 , g_2 and g_3). The zigzag lines represent the interchain one-particle hopping, t_{\perp} , from the i -th chain to the nearest-neighbor chain. The white and black squares represent the interchain AF interactions, J and K , in the normal and umklapp channels, respectively. i and j denote different chain indices.

We consider quenched randomness, where the free energy is averaged over random potentials by the replica trick, $\ln Z = \lim_{N \rightarrow 0} (Z^N - 1)/N$, for the partition function, Z . Here N identical replicas are introduced with indices, $\alpha = 1, 2, \dots, N$. We take an average $\langle Z^N \rangle_{\text{random}}$ for integer N , continue the result analytically to real N , and finally take the $N \rightarrow 0$ limit.

RENORMALIZATION-GROUP EQUATIONS

Based on the bandwidth cutoff regularization scheme, we parameterize the temperature as $T = E_0 e^{-l}$ with the scaling parameter l . As l goes from zero to infinity, we move from high-temperature scales, where the system is re-

garded as collection of isolated 1D chains, to low-temperature scales, where the interchain coupling is substantial. Performing a scale transformation at the two-loop level and re-expressing the renormalized action at $l + dl$ in terms of the renormalized coupling strengths, we obtain RG equations,

$$d\tilde{g}_1/dl = w_1 - 2\theta\tilde{g}_1 - \tilde{D}_\xi, \quad (3)$$

$$d\tilde{g}_2/dl = w_2 - 2\theta\tilde{g}_2 - \tilde{D}_\eta, \quad (4)$$

$$dg_3/dl = w_3 - 2\theta g_3, \quad (5)$$

$$d\tilde{D}_\eta/dl = w_\eta + (1 - 2\theta)\tilde{D}_\eta, \quad (6)$$

$$d\tilde{D}_\xi/dl = w_\xi + (1 - 2\theta)\tilde{D}_\xi, \quad (7)$$

$$d \ln t_\perp / dl = 1 - \theta, \quad (8)$$

$$dJ/dl = -(\tilde{g}_2^2 + 4g_3^2)\tilde{t}_\perp^2/2 + \tilde{g}_2 J/2 + 2g_3 K - J^2/4 - K^2, \quad (9)$$

$$dK/dl = -2\tilde{g}_2 g_3 \tilde{t}_\perp^2 + 2(\tilde{g}_2 K + g_3 J) - JK, \quad (10)$$

where $\tilde{D}_\xi = D_\xi \Lambda / 2v_F$, $\tilde{D}_\eta = D_\eta \Lambda / 2v_F$, $\tilde{g}_1 = g_1 - \tilde{D}_\xi$, $\tilde{g}_2 = g_2 - \tilde{D}_\eta$ and $\tilde{t}_\perp = t_\perp / E_0$. Λ is the length scale which characterizes inelastic scattering processes between different replicas. The two-loop vertex correction diagrams for \tilde{g}_1 , \tilde{g}_2 , g_3 , \tilde{D}_η and \tilde{D}_ξ give w_1 , w_2 , w_3 , w_η and w_ξ , respectively, and the two-loop self-energy diagrams give θ . The contribution of the diagrams containing a loop connected to outer lines via the random scattering as shown in Fig. 2 is proportional to the number of replicas, N , and vanishes in the replica limit, $N \rightarrow 0$.

FIGURE 2 A diagram which vanishes in the replica limit, $N \rightarrow 0$. Note that the replica index of the internal loop, γ , runs from 1 to N .

PHASE DIAGRAMS

Based on the RG flows obtained through solutions of Eqs. (3) – (10), we introduce the three characteristic scales, l_{loc} , l_{FL} and l_{AF} :

$$\tilde{D}_\xi = 1 \quad \text{at } l = l_{\text{loc}}, \quad (11)$$

$$t_\perp / E_0 = 1 \quad \text{at } l = l_{\text{FL}}, \quad (12)$$

$$K = -\infty \quad \text{at } l = l_{\text{AF}}. \quad (13)$$

l_{loc} is the scale which characterizes the crossover to the Anderson localization phase. We call this phase a “one-dimensional Anderson localization (1DAL) phase,” since the one-dimensional scaling procedure works during the crossover. l_{FL} is the scale which characterizes the crossover to the three-dimensional FL phase with randomness. l_{AF} is the scale at which there occurs the phase transition to the AF phase from the ICM phase. We solve the coupled RG equations, (3) – (10), and check which of Eqs. (11) – (13) is satisfied at the highest energy scales, depending on the initial values of the coupling strengths, and obtain phase diagrams which are classified into the following three categories.

FIGURE 3 Phase diagrams of the system. **ICM**=incoherent metal phase. **AF**=antiferromagnetic phase. **1DAL**=one-dimensional Anderson localization phase. **FL**=Fermi liquid phase.

I. Competition between the AF phase and the 1DAL phase [Fig.3(a)]

For $U = 0.3\pi v_F$, $\tilde{D}_{\eta;0} = 0.01$ and $t_{\perp;0} = 0.01E_0$, we obtain Fig.3(a) on the plane of the initial random backward scattering strength, $\tilde{D}_{\xi;0}$, and the temperature. Owing to the strong umklapp scattering and the weak inter-chain one-particle hopping, the low temperature phases are determined by the competition between the AF coherence and the 1DAL. We see that the AF transition temperature, T_N , increases with $\tilde{D}_{\xi;0}$, since during the renormalization process growth of \tilde{D}_{ξ} suppresses \tilde{g}_1 and enhances g_3 . Growth of

the umklapp scattering plays an essential role for the AF transition from the ICM phase^[4].

II. Competition between the 1DAL phase and the FL phase [Fig.3(b)]

For $U = 0.05\pi v_F$, $\tilde{D}_{\eta;0} = 0.01$ and $\tilde{D}_{\xi;0} = 0.2$, we obtain Fig.3(b) on the plane of the initial interchain one-particle hopping integral, $t_{\perp;0}$, and the temperature. Owing to the weak umklapp scattering and the strong random backward scattering, the low temperature phases are determined by the competition between the 1DAL and the interchain one-particle coherence.

III. Competition between the AF phase and the FL phase [Fig.3(c)]

For $U = 0.5\pi v_F$, $\tilde{D}_{\eta;0} = 0.08$ and $\tilde{D}_{\xi;0} = 0.08$, we obtain Fig.3(c) on the plane of $t_{\perp;0}$ and the temperature. Owing to the strong umklapp scattering and the weak random backward scattering, the low temperature phases are determined by the competition between the AF coherence and the interchain one-particle coherence.

Finally, it should be noted that even inside the AF and FL phases in Figs.3(a)-(c), the randomness effects would work. This issue is beyond the scope of the present RG approach.

Acknowledgments

This work was supported by a Grant-in-Aid for Encouragement of Young Scientists from the Ministry of Education, Science, Sports and Culture, Japan.

References

- [1]T.Giamarchi and H.J.Schulz, *Phys. Rev. B* **37**, 325 (1988).
- [2]S.Fujimoto and N.Kawakami, *Phys. Rev. B* **54**, 11018 (1996).
- [3]C.Bourbonnais, in *Strongly Interacting Fermions and High Tc Superconductivity*, ed. B.Doucot and J.Zin-Justin (Elsevier, 1995), p.307.
- [4]J.Kishine and K.Yonemitsu, *J. Phys. Soc. Jpn.* **67**, 2590 (1998); J.Kishine and K.Yonemitsu, *J. Phys. Soc. Jpn.* **68**, No.8 (1998).

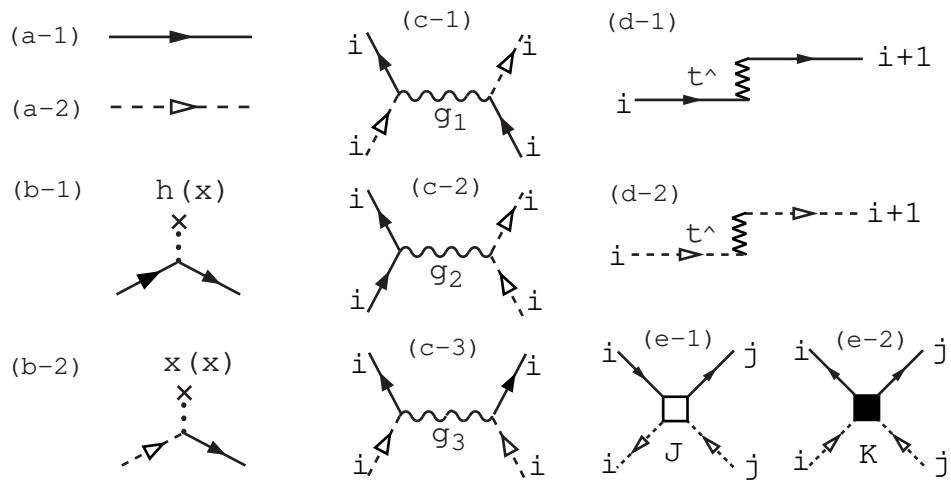


Fig.1

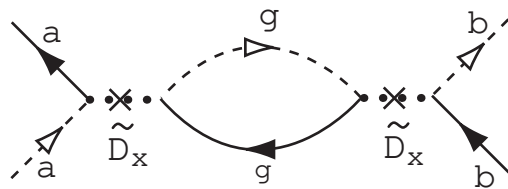


Fig.2

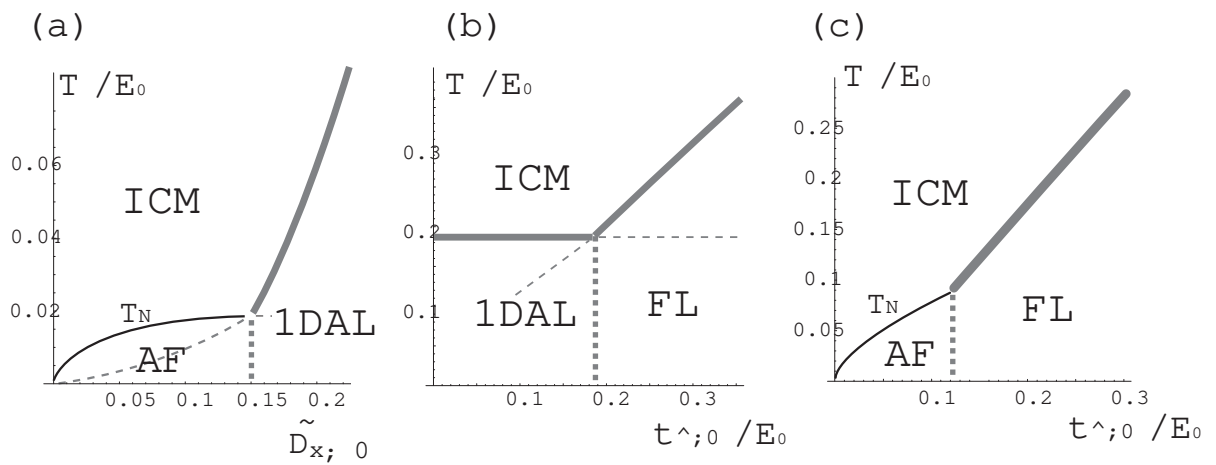


Fig.3